

---

1                    Characteristics of cloud-to-ground (CG) lightning and  
2                    differences between +CG and -CG in China regarding CNLDN  
3                    network

4                    **Ruijiao Jiang<sup>a</sup>, Guoping Zhang<sup>a,\*</sup>, Shudong Wang<sup>a</sup>, Bing Xue<sup>a</sup>, Zhengshuai Xie<sup>b</sup>,**  
5                    **Tingzhao Yu<sup>a</sup>, Kuoyin Wang<sup>a</sup>, Jin Ding<sup>a</sup>, Xiaoxiang Zhu<sup>a</sup>**

6                    <sup>a</sup> Public Meteorological Service Center, China Meteorological Administration, Beijing 100081, China

7                    <sup>b</sup> Weather Modification Centre, China Meteorological Administration, Beijing 100081, China

8                    \*Corresponding author. E-mail address: [zhanggp@cma.gov.cn](mailto:zhanggp@cma.gov.cn)

9                    **Abstract**

10                    The lightning location system consisting of multiple ground-based stations is an  
11                    effective means of lightning observation. The dataset from CNLDN (China National  
12                    Lightning Detection Network) in 2016-2021 is employed to analyze the temporal and  
13                    spatial lightning distributions and the differences between +CG (cloud-to-ground  
14                    lightning) and -CG flashes in China. On the monthly scale, lightning activity is most  
15                    prevalent during the summer months (June, July, and August), accounting for 70.7% of  
16                    the year. Spring sees more lightning than autumn, and winter has only a small amount  
17                    in southeastern coastal areas. During the day, the frequency of lightning peaks at 15:00-  
18                    17:00 CNT and is lowest at 8:00-11:00 CNT. For the period with high CG frequency  
19                    (summer of a year or afternoon of a day), the proportion of +CG flashes and the  
20                    discharge intensity is relatively small. Winter in a year and morning or midnight in a  
21                    day correspond to a greater +CG proportion and discharge current. Spatially, low  
22                    latitude, undulating terrain, seaside, and humid surface are favorable factors for  
23                    lightning occurrence. Thus, the southeast coastland has the largest lightning density,  
24                    while the northwest deserts and basins and the western and northern Tibetan Plateau  
25                    with altitudes over 6000 meters have almost no lightning. The proportion of +CG  
26                    flashes and the discharge intensity are low in the southern region with high lightning  
27                    density but diverse in other regions. The Tibetan Plateau leads to the complexity of  
28                    lightning activity in China and lays the foundation for studying the impact of surface  
29                    elevation on lightning. Results indicate that the +CG ratio on the eastern and southern  
30                    Tibetan Plateau is up to 15%, larger than the plain regions. The current of -CG is  
31                    positively correlated with altitude, but +CG shows a negative correlation, resulting in a  
32                    large difference in current between +CG and -CG on the plain and approach on the  
33                    plateau.

34                    **Keywords:** China, CNLDN, Lightning characteristics, +CG flashes, Current peak

---

35 value

## 36 1. Introduction

37 Most lightning is generated mainly through meso-small scale severe convective  
38 weather, with few occurring in stratus clouds and tropical cyclones and occasionally  
39 during volcanic eruptions, nuclear explosions, and dust storms (Rakov and Uman,  
40 2003). Lightning, a violent long-distance transient discharge phenomenon, could cause  
41 severe disasters such as human and animal casualties, forest fires, and electronic and  
42 communication equipment interruptions. Lightning is also associated with extreme  
43 weather events such as heavy rainfall, hail, and strong winds. These events can cause  
44 damage to infrastructure, crops and property, and pose a threat to public safety.  
45 Therefore, advanced lightning monitoring technology is necessary for the development  
46 of lightning science and also scientific protection against meteorological disasters.

47 Lightning discharge emits electromagnetic spectrums with a broad range,  
48 providing an essential avenue for lightning detection. The very low frequency / low  
49 frequency (VLF/LF, 20-300 kHz) band radiation is mainly produced by the cloud-to-  
50 ground (CG) return strokes, intracloud (IC) K-changes, and other discharge processes  
51 with a large spatial scale (Preston and Tolver, 1989; Schulz et al., 2016; Cummins et al.,  
52 1998). VLF/LF electromagnetic waves could propagate along the ground surface or be  
53 reflected between the surface and ionosphere propagation, with the superiority of long  
54 propagation distance (hundreds to thousands of kilometers) and slow attenuation. This  
55 frequency range thus is suitable for large-scale lightning detection and is currently the  
56 most commonly used target detection band for ground-based lightning location  
57 systems (Wang et al., 2020).

58 Representative examples of modern lightning location systems working in  
59 VLF/LF band are mainly the U.S. National Lightning Detection Network (NLDN), Los  
60 Alamos Sferic Array (LASA), European Cooperation for Lightning Detection  
61 (EUCLID), etc. The three nationwide detection networks in China are China National  
62 Lightning Detection Network (CNLDN), operated by the Meteorological Observation  
63 Centre of China Meteorological Administration (CMA), the Lightning Location System  
64 (LLS) of the State Grid Corporation of China, and the Three-Dimensional Lightning  
65 Location System (3D-LLS) deployed by the Institute of Electrical Engineering of  
66 Chinese Academy of Sciences (CAS). There are also small-scale and refined detection  
67 systems in local China areas, such as the Beijing Lightning Network (BLNET)  
68 established by the Institute of Atmospheric Physics of CAS, the Guangdong-  
69 Hongkong-Macao Lightning Location System (GHMLLS) deployed by the  
70 meteorological departments of Guangdong Province, Hongkong, and Macao.

71 China spans a wide range of latitudes from north to south and significant terrain  
72 changes from east to west. The western and northern parts of the Tibetan Plateau have  
73 large uninhabited areas with altitudes above 4500 m. The above factors pose challenges  
74 for the installation of lightning detectors and the improvement of the accuracy of

---

75 locating algorithms. Currently, most of the analyses of lightning characteristics in China  
76 are based on lightning imagers on satellites and the World-Wide Lightning Location  
77 Network (WWLLN)(Ma et al., 2005; You et al., 2019; Ma et al., 2021). However, the  
78 Optical Transient Detector (OTD) on Microlab-1 and Lightning Imaging Sensor (LIS)  
79 on TRMM was no longer updated, and the Chinese Lightning Mapping Imager (LMI)  
80 on FY-4A is not oriented to the China area all year round. Meanwhile, the detection rate  
81 of the satellite sensor and WWLLN is low and not valuable for analyzing the difference  
82 between different types of flashes. CNLDN is nowadays the most widely used system  
83 by the meteorological departments in China and has accumulated observational data for  
84 many years. Lightning studies based on CNLDN data are currently relatively limited  
85 and generally focus on localized areas(Liu et al., 2021; Li et al., 2020).

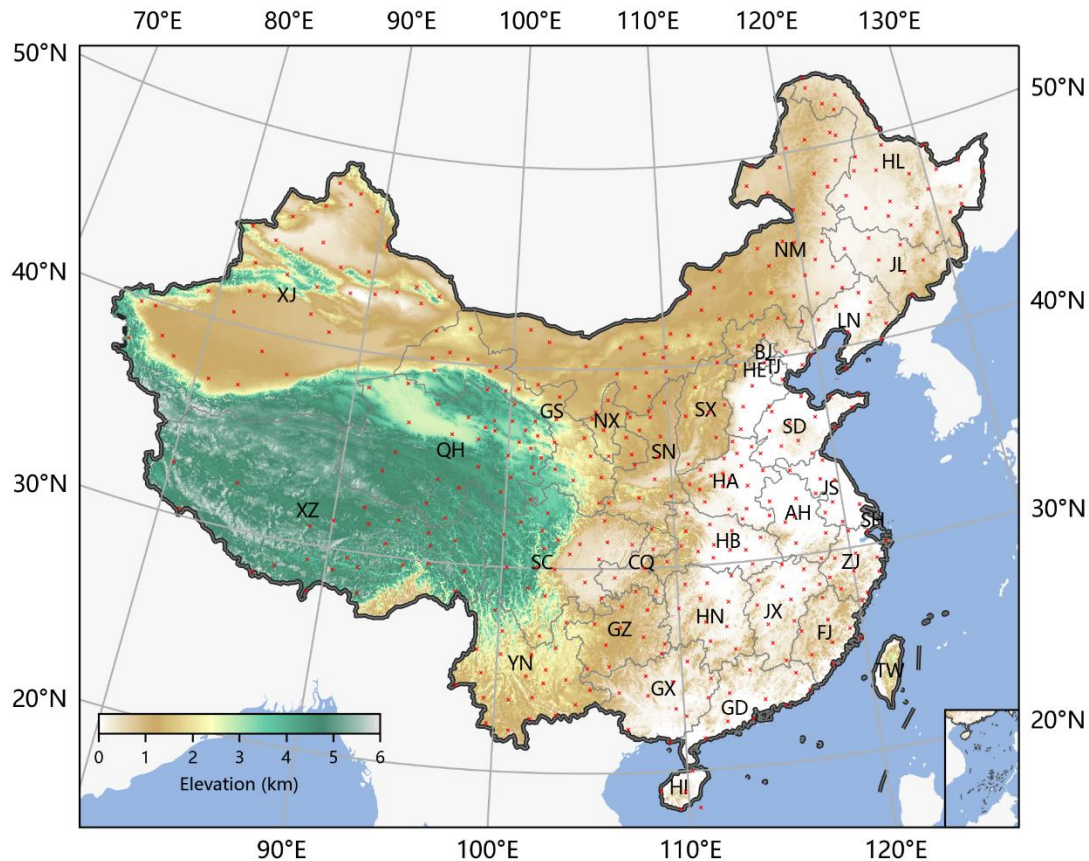
86 This study makes use of CNLDN data from 2016-2021 to analyze the lightning  
87 climate over China by dividing the continental region into four blocks. We also focus  
88 on comparing the differences between +CG and -CG flashes regarding temporal and  
89 spatial distribution. In addition, China's wide latitude and longitude range and complex  
90 topography make for our studying the relationship between lightning and geographic  
91 factors.

## 92 2. Data source

93 CNLDN was initially developed in 2007 by the National Space Science Center  
94 (NSSC) of CAS and is now operated by the Meteorological Observation Centre of  
95 CMA. The system comprised 435 sub-stations (as of 2020), each equipped with a  
96 lightning detector, and a central data processing station located at the National  
97 Meteorological Information Center. Although with some blind areas in Xinjiang and  
98 Xizang, CNLDN can generally achieve nationwide lightning detection. The distribution  
99 of sub-stations can be seen in Fig. 1.

100 The network uses a time-of-arrival (TOA) technique, with a GPS timing error of  
101 fewer than 20 ns (in clear sky conditions), to detect VLF/LF pulses of CG return strokes.  
102 A lightning flash may consist of several CG strokes, and the system groups single-point  
103 signals to a flash event based on their separation in time and space. Return strokes  
104 within a 500 ms time interval and 10 km distance interval are classified as a single CG  
105 flash, with the first detected stroke representing the entire flash.

106 In this study, we analyze lightning characteristics in inland China using the  
107 CNLDN dataset from 2016-2021, downloaded from the CMA big data cloud platform.  
108 For each flash, we can obtain information on the time of occurrence, latitude, longitude,  
109 current peak value, and the number of triggered stations.



110

111 **Fig. 1. CNLDN sites distribution and altitude distribution map of China with the location of each province**  
 112 **and municipality (indicated by abbreviations, for details, refer to:**

113

*<https://www.iso.org/obp/ui/#iso:code:3166:CN>*

### 114 3. CG flash characteristics of China

115 China's climate features are greatly influenced by its wide latitudinal span,  
 116 significant terrain disparity, complex topography, and ocean currents (Ren et al., 2012).  
 117 Lightning is a fundamental meteorological element, and its long-term accumulation  
 118 characteristics are closely linked to China's climate. The spatial distribution of lightning  
 119 in China is determined by a combination of factors, including atmospheric circulation,  
 120 topography, distance from the sea, latitude, etc.

#### 121 3.1 CG distribution in China

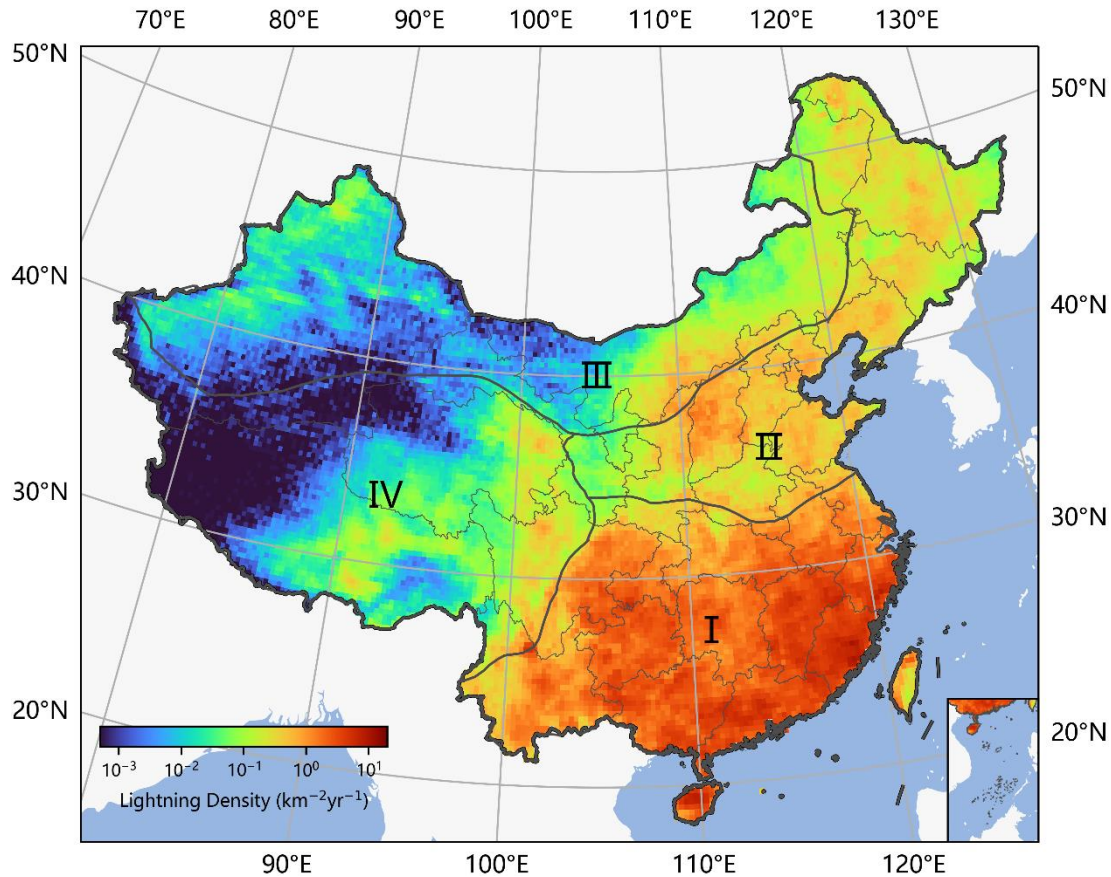
122 Previous studies have often divided China into four major geographical regions,  
 123 each with relatively uniform climatic characteristics. These regions are Southern China  
 124 (Region-I), Northern China (Region-II), Northwestern China (Region-III), and the  
 125 Qinghai-Tibet region of China (Region-IV), as illustrated in Fig. 2. The Qinling  
 126 Mountains-Huaihe River line, which roughly coincides with the 0 °C isotherm and 800  
 127 mm annual precipitation line in January, serves as the boundary between Region-I and

---

128 Region-II. The Daxing'an Mountains-Yinshan Mountains-Helan Mountains, which  
129 divide the monsoon and non-monsoon regions and the 400 mm annual precipitation  
130 line, serve as the boundaries between Region-II and Region-III. The boundary between  
131 Region-IV and Regions I-II-III is approximately the line between China's first and  
132 second steps in terrain.

133 Fig. 2 displays the distribution of annual average CG flash density from 2016-  
134 2021. Lightning primarily occurs in convective precipitation and, to a lesser extent, in  
135 stratus cloud precipitation. Generally, the spatial distribution of lightning is consistent  
136 with the distribution of annual average precipitation in China, as illustrated in Fig. 3 in  
137 Jin et al. (2021).

138 Region-I has the highest concentration of CG flashes, with a density greater than  
139  $1 \text{ km}^{-2} \text{ yr}^{-1}$ . The leap line of lightning density corresponds well with the  $0 \text{ }^{\circ}\text{C}$  isotherms  
140 in January, the 800 mm annual equivalent precipitation line, and the eastern dividing  
141 line of the first and second terrain steps. The climate in Region-I is mainly influenced  
142 by the tropical/subtropical monsoon. The southeast monsoon from the Pacific Ocean  
143 and the southwest monsoon from the Indian Ocean make the summer hot and humid,  
144 and prone to thunderstorms. In particular, the monsoon influence is more pronounced  
145 in coastal areas with abundant water vapor and thermal conditions. In the mountainous  
146 regions of Hainan, Guangdong, Fujian, and Zhejiang, where the rolling topography lifts  
147 the warm and humid air masses, thunderstorm activity is most frequent, resulting in  
148 high lightning density. Although the Sichuan Basin and Yunnan are far from the  
149 coastline, they are located at the eastern and southern windward slopes of the Tibetan  
150 Plateau, which benefits the generation of thunderstorm activities due to the topographic  
151 uplift.



152  
153  
154  
155

**Fig. 2. 2016-2021 annual average CG flash density distribution in China. Region-I: Southern China; Region-II: Northern China; Region-III: Northwestern China; Region-IV: Qinghai-Tibet region of China. The grid size is  $0.25^\circ \times 0.25^\circ$ .**

156  
157  
158  
159  
160  
161  
162  
163  
164  
165  
166  
167

Region-II has a temperate monsoon climate, with summer influenced by the southeast monsoon carrying temperate marine air mass or degenerate tropical marine air mass, making summer warm and rainy. Most areas have CG flash density between  $0.1-1 \text{ km}^{-2} \text{ yr}^{-1}$ , slightly lower than Region-I. The lightning density in Region-II is also greater in the seaside area than inland areas. Shanxi is located in a mountainous region, and the undulating terrain makes it a high incidence area for thunderstorm activity. Region-II has the most extensive plain, Northeastern China Plain, surrounded by the Daxing'an Mountains-Xiaoxing'an Mountains-Changbai Mountains. The landform is conducive to the southeast monsoon to reach the inland areas of Region-II and form summer thunderstorms. Jilin is only a dozen kilometers from the Sea of Japan, facilitating the entry of Japanese warm air currents. Therefore, despite its high latitude, thunderstorm activity is relatively intense in Region-II.

168  
169  
170  
171  
172  
173

Region-III, which includes Xinjiang, northern Gansu, and most of Inner Mongolia, has a temperate continental climate. The southern and central parts of Region-III consist mostly of vast deserts and gobies. The Tibetan Plateau blocks the humid South Asian monsoon, and its arid surface cannot produce abundant water vapor, resulting in few thunderstorms. However, the Tianshan Mountains, Kunlun Mountains, Altay Mountains, and Tarbahatai Mountains located in the hinterland of the Eurasian

---

174 continent, are provided with water vapor for thunderstorm generation through the  
175 westerly circulation that transports evaporated water vapor from the Atlantic Ocean and  
176 the Eurasian continent. As a result, the northern mountainous areas occupy almost all  
177 the lightning activity in Xinjiang. The southeastern monsoon flowing through Region-  
178 II can also bring some thunderstorm processes to the eastern and central mountainous  
179 regions in Inner Mongolia during summer.

180 Region-IV's primary landmass is the Tibetan Plateau, which includes Tibet,  
181 Qinghai, southern Xinjiang, and western Sichuan. It has a highland mountain climate,  
182 and the overall geomorphic distribution trend increases from east to west (Ma et al.,  
183 2021). The uninhabited areas above 4500 meters in elevation in the west and north of  
184 Region-IV are icy all year round, covered by snow and glaciers. The Qaidam Basin in  
185 Qinghai is a closed, huge, interrupted basin, where dry sinking airflow from the  
186 northern edge of the plateau in summer leads to water shortage. Consequently, there are  
187 few thunderstorm activities in these areas, and the distribution of sub-stations is sparse,  
188 making them the regions with the lowest lightning density detected in China, with CG  
189 flash density less than  $10^{-3} \text{ km}^{-2} \text{ yr}^{-1}$ . In contrast, the southern Himalayas, near the  
190 Yarlung Tsangpo River Grand Canyon, has a relatively low altitude, opening a "gap"  
191 for the influx of abundant water vapor from the Bay of Bengal. However, this narrow  
192 plain area, located in Mêdog County, has very high precipitation but low lightning  
193 density, which can also be concluded from the observations of TRMM. The remaining  
194 moisture continues northward across this plain, causing most thunderstorms between  
195 the east-west Himalayas Mountains and Tanggula Mountains. The thunderstorms on  
196 the east side of the plateau are mainly influenced by the low vortex and the shear line,  
197 which is usually stable at around  $32.5^{\circ}\text{N}$ (You et al., 2019; Qie et al., 2003). The high  
198 lightning density area is precisely located on the south side of the shear line.

### 199 3.2 Differences between +CG and -CG

200 Based on the different polarities of neutralized charges in thunderclouds, CG can  
201 be classified into two types: +CG and -CG. Generally, +CG has a lower occurrence  
202 probability, accounting for only about 10% of all CG, but it is characterized by a larger  
203 spatial scale and charge transfer, which results in a more significant hazard (Preston  
204 and Tolver, 1989; Carey and Buffalo, 2007). Studies have suggested that thunderstorms  
205 dominated by +CG are more likely to result in tornadoes and hail, particularly if the  
206 dominant phase lasts for tens of minutes. This may be related to changes in the charge  
207 distribution structure within thunderstorm clouds during extreme weather  
208 events(Williams, 1985). Previous research has been conducted on the comparative  
209 analysis of +CG and -CG in specific regions (Nag et al., 2014; Rakov and Uman, 2003).  
210 Based on these findings, this study aims to further investigate the spatial and temporal  
211 variability of +CG and -CG in China, taking into account the complex climatic and  
212 geographical factors that influence lightning activity.

---

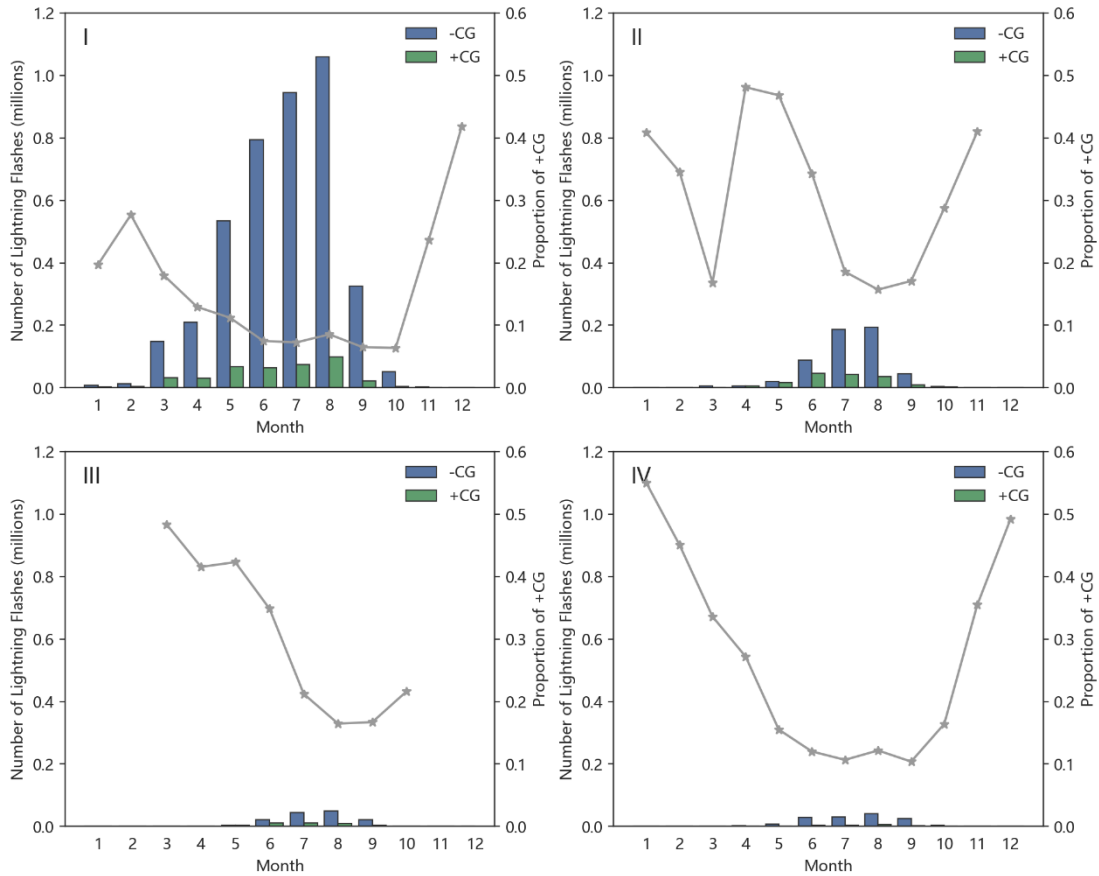
### 213 3.2.1 Comparison of the temporal distribution of +CG and -CG

214 The geographical and climatic features differ considerably across the four regions.  
215 Therefore, we analyze the temporal distribution of lightning separately for each region.

216 Fig. 3 illustrates the monthly average CG flash frequency distribution in China  
217 over a six-year period from 2016 to 2021. The lightning frequency varies significantly  
218 across the four regions, with Region-I having the highest frequency, followed by  
219 Region-II and Region-III, and Region-IV having the lowest frequency. But the lightning  
220 frequency shows similar fluctuations throughout the year between the regions, with  
221 August having the highest frequency and December having the lowest. Lightning  
222 activity is also scarce in November, January, and February, with a sudden surge in  
223 March and a gradual increase in the following months. Based on the seasonal  
224 classification, lightning activity is most active in summer (June, July, and August),  
225 accounting for 70.7% of the year. In other seasons, lightning is more frequent in spring  
226 (19.1%) than in autumn (9.8%), but much less frequent than in summer. This is mainly  
227 because the summer monsoon affecting China starts to form during April and May,  
228 while the cold and dry winter monsoon starts to build up and push southward from  
229 September, making thunderstorm activity in spring and autumn mainly concentrated in  
230 southern areas, particularly coastal areas. In winter, most regions in China are  
231 controlled primarily by cold high pressure, resulting in very little lightning, with only  
232 a small amount occurring in southeastern coastal areas, accounting for just 0.4% of the  
233 year. Overall, lightning distribution follows a seasonal trend that advances from south  
234 to north and then retreats southward, which is consistent with the trend of the summer  
235 monsoon.

236 Furthermore, the proportion of +CG flashes in different months is calculated and  
237 represented by the gray line in Fig. 3. To ensure the reliability of the analysis, months  
238 with less than 50 +CG flashes are excluded to avoid the impact of outliers. Results  
239 indicate an evident inverse relationship between the proportion of +CG flashes and the  
240 frequency of lightning. Notably, the three months with the highest incidence of CG  
241 flashes, namely July, August, and September, exhibit the lowest proportion of +CG  
242 flashes across the four regions. During this period, Region-I and Region-IV, located at  
243 lower latitudes, exhibit a proportion of +CG flashes of approximately 0.1, while  
244 Region-II and Region-III display proportions of around 0.2. In other months, some  
245 irregular fluctuations are observed, among which Region-IV has rare thunderstorms in  
246 winter but demonstrates the highest proportion of +CG flashes, reaching 0.55.  
247 Moreover, Regions I and II show significantly high proportions of +CG flashes in  
248 February and April-May, respectively.

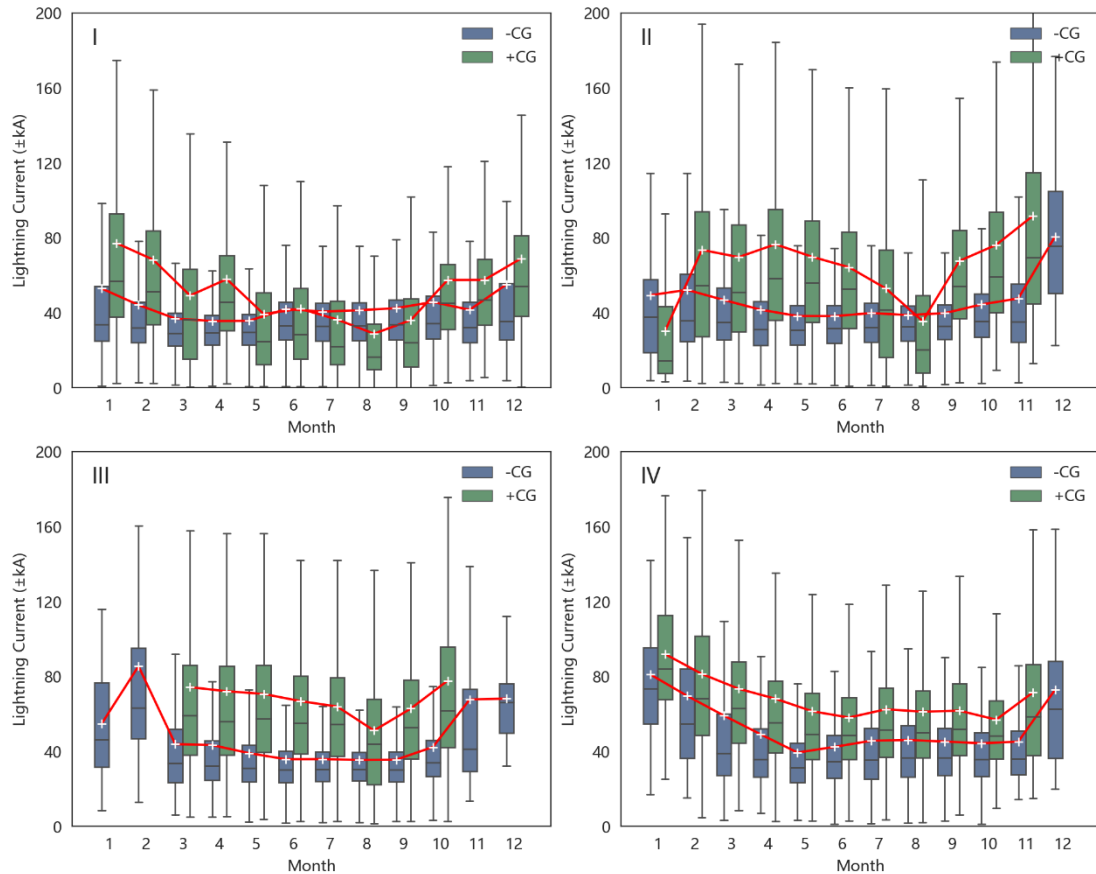




249  
250  
251

**Fig. 3. Monthly variation of the frequency distribution of +CG and -CG flash. The gray line represents the proportion of +CG flash.**

252 Fig. 4 illustrates the analysis of the current peak value of two types of CG flashes  
253 in different months and regions. To avoid outliers, no box is drawn when the flash count  
254 is less than 50. Overall, the distribution range is wider in winter than in other seasons,  
255 and Region-II has a wider current distribution interval than other regions. The average  
256 current peak value of each month is indicated by a white cross, and the variation trends  
257 are shown by red lines. The results indicate that +CG flashes generally have a higher  
258 discharge intensity than -CG flashes. The discharge intensity and the proportion of +CG  
259 flashes exhibit similar trends, with a higher proportion and stronger discharge intensity  
260 in winter and a lower proportion and weaker discharge intensity in summer. In Region-  
261 I and Region-II, the seasonal fluctuations of +CG current are more pronounced than -  
262 CG current, with the current of +CG falling even below -CG in August. The trends of  
263 +CG and -CG flash discharge intensity are more consistent in Regions-III and Region-  
264 IV.



265  
266  
267

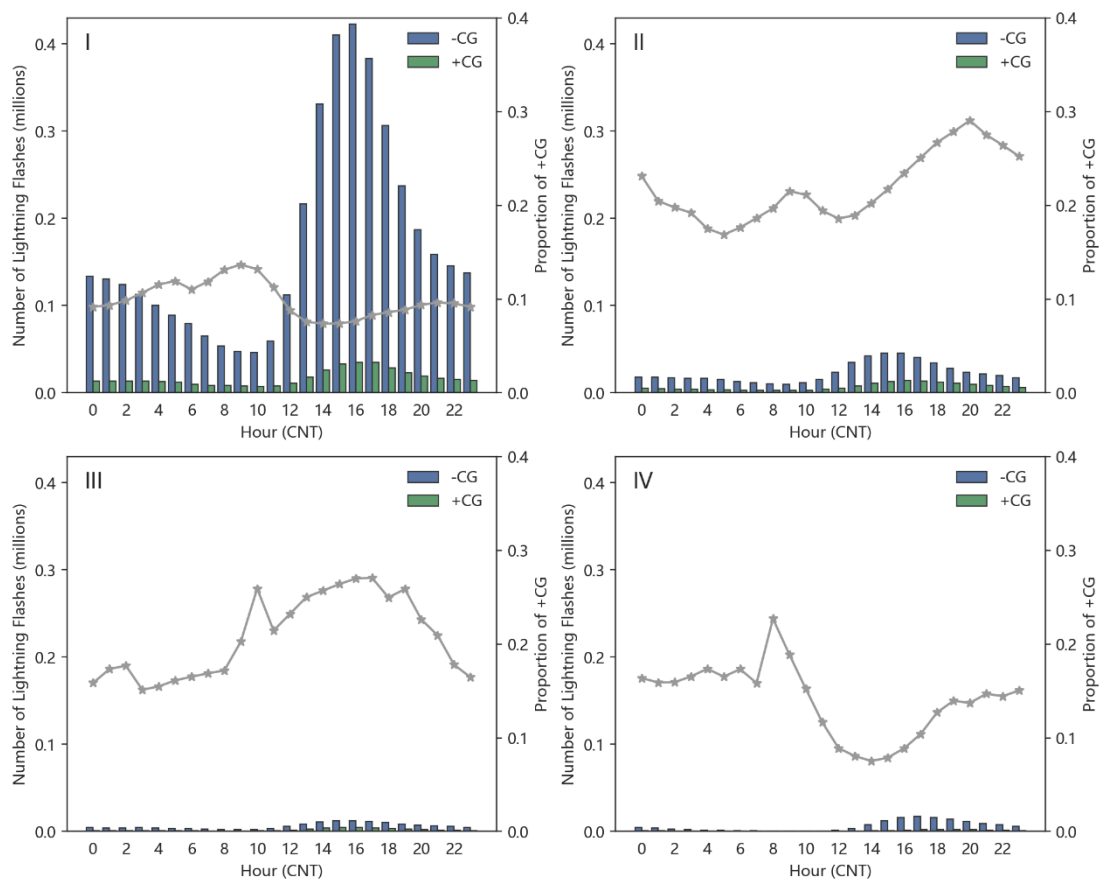
**Fig. 4. Monthly variation of the peak current distribution of +CG and -CG flash. The red line represents the average peak current of each month. The -CG flash current is expressed in absolute value.**

268  
269  
270  
271  
272  
273  
274  
275  
276  
277

Fig. 5 illustrates the hour-by-hour frequency and intensity variations of CG flashes throughout the day. The frequency of both +CG and -CG flashes shows noticeable and consistent fluctuations. The active period for lightning activity is concentrated in the late afternoon to midnight, which coincides with the maximum accumulation of radiative heating and vapor conducive to the development of convection, particularly during summer thunderstorms in China. Lightning frequency peaks at 15:00 CNT (UTC+8) in Region-I and Region-II in the east of China and 1-2 hours later in Region-III and Region-IV in the west of China. After nightfall, lightning activity gradually weakens due to the decline in unstable energy, dropping to a trough at 8:00-10:00 CNT the following day.

278  
279  
280  
281  
282  
283  
284  
285  
286

The proportion of +CG flashes is inversely correlated with the total number of CG flashes in a day, as shown in Fig. 5. The maxima of the +CG proportion coincides with the lowest lightning frequency at 8:00-10:00 CNT in all four regions, but the minima appear 2-3 hours earlier than the frequency peak at 16:00 CNT. Region-I and Region-IV at low latitudes have maximum proportions in the morning, while Region-II and Region-III at high latitudes have maximum proportions in the evening. Additionally, the proportion of +CG flashes is lower in Region-I and Region-IV, with minimums of less than 0.1, than in Region-II and Region-III, where peak values can reach 0.3. These findings demonstrate a close relationship between thunderstorm characteristics and



288

289

290

**Fig. 5. Hourly variation of the frequency distribution of +CG and -CG flash. The gray line represents the proportion of +CG flash. The time zone is CNT (UTC+8).**

291

292

293

294

295

296

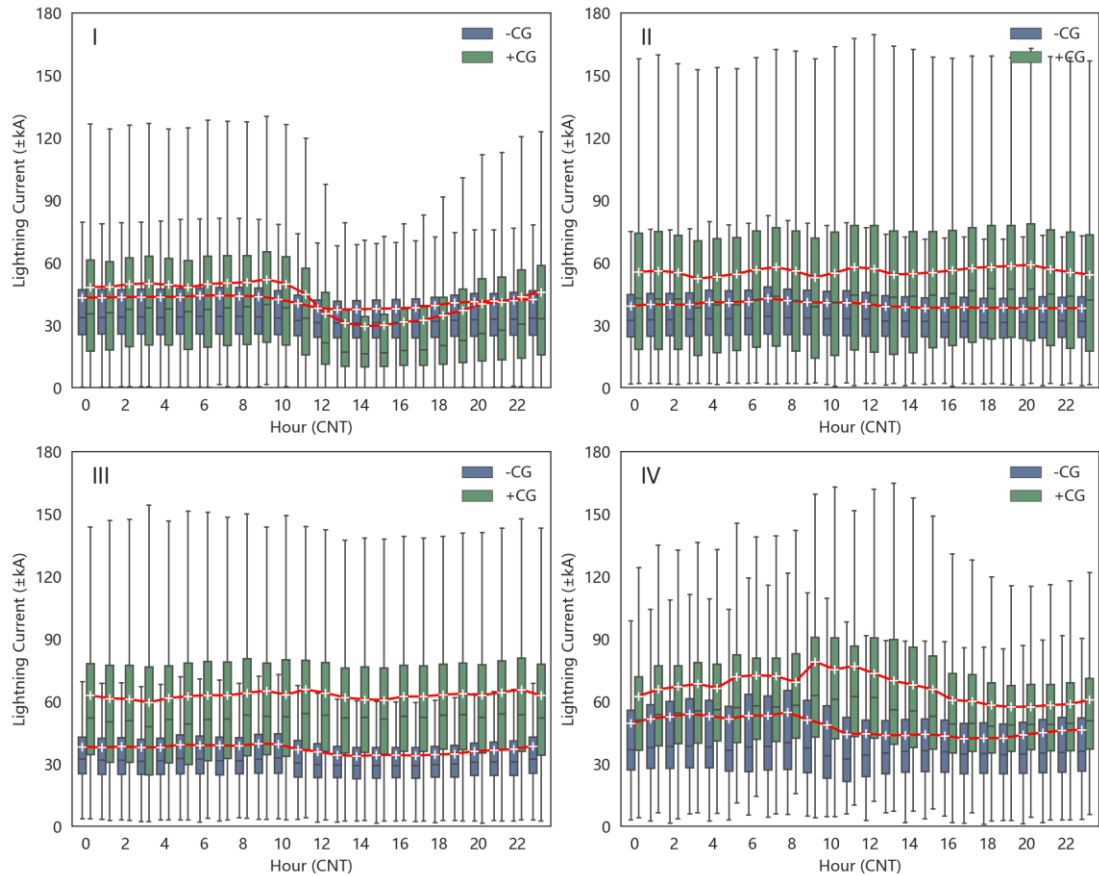
297

298

299

300

The hourly current peak value distribution and their averages of +CG and -CG flashes are shown in Fig. 6. Region-II and Region-III, located at higher latitudes, have a wider distribution range of peak currents. But their variation is relatively stable, while the current of +CG in Region-III is slightly larger than in Region-II. The current in Region-1 decreases significantly in the noon and afternoon, with a more intense change in -CG than in +CG, resulting in the absolute current of two types of flashes even being reversed. Meanwhile, Region-IV, which has complex terrain due to the Qinghai-Tibet Plateau, exhibits intricate current variations, with an increase in +CG and a decrease in -CG. As a result, there is a huge disparity in current between the two types of flashes during noon and afternoon.

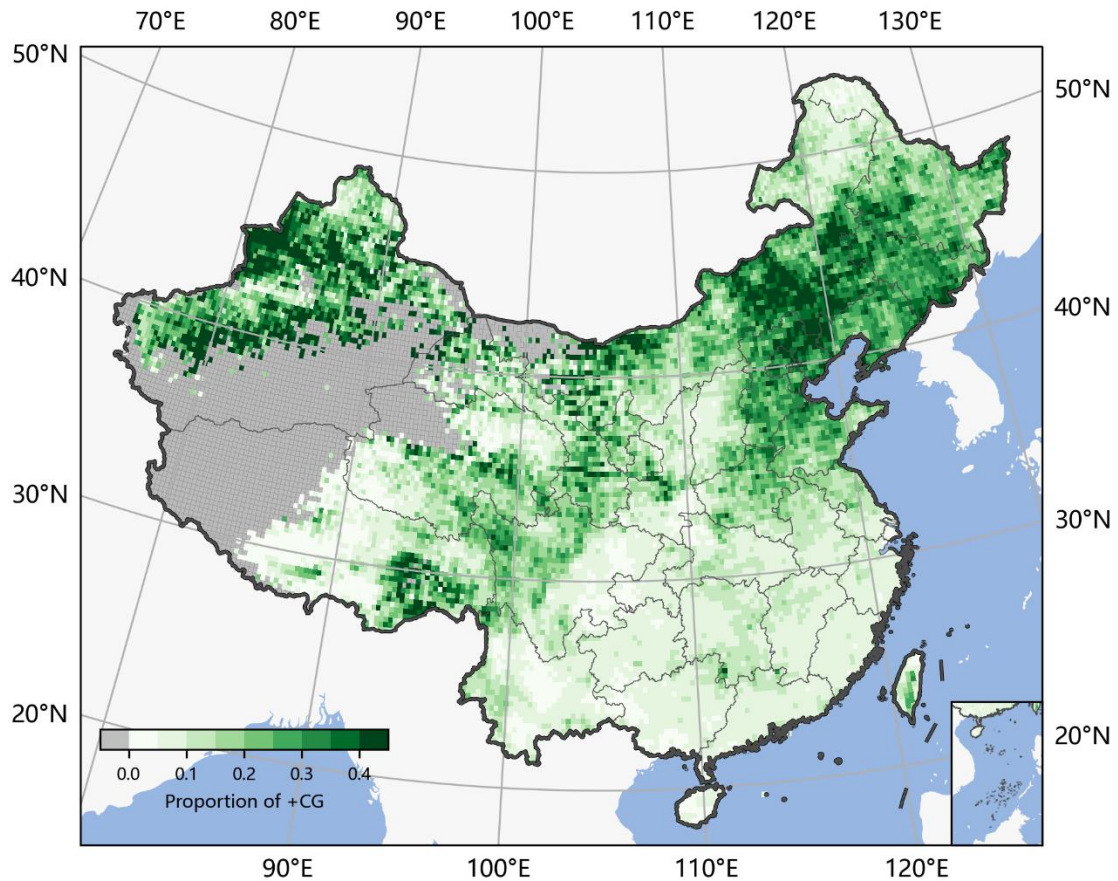


301  
302  
303  
304

**Fig. 6. Hourly variation of the peak current distribution of +CG and -CG flash. The red line represents the average peak current of each month. The -CG flash current is expressed in absolute value. The time zone is CNT (UTC+8).**

### 305 3.2.2 Comparison of the spatial distribution of +CG and -CG

306 The geography of China is characterized by its complexity, and this is reflected in  
307 the variability of the ratio of +CG and -CG flashes across different regions. Fig. 7  
308 illustrates the spatial distribution of the proportion of +CG flashes, with gray areas  
309 indicating grids with less than 50 CG flashes accumulated over a 6-year period. These  
310 grids are mainly located in the central, western, and northern parts of Tibet and the  
311 western and southern parts of Xinjiang. Region-I, which has the highest density of CG  
312 flashes, has a low proportion of +CG flashes, at less than 10%. Conversely, the other  
313 three regions have a higher proportion of +CG flashes, particularly the North China  
314 Plain and adjacent Inner Mongolia, as well as some parts of Region-III, where the +CG  
315 proportion can reach 30-40%. The proportion of +CG flashes in Shanxi and Shaanxi,  
316 both located in Region-II, is lower than in other regions of the same area. Overall,  
317 regions with lower CG flash density tend to have a higher proportion of +CG flashes,  
318 and high latitudes correspond to a higher +CG proportion.

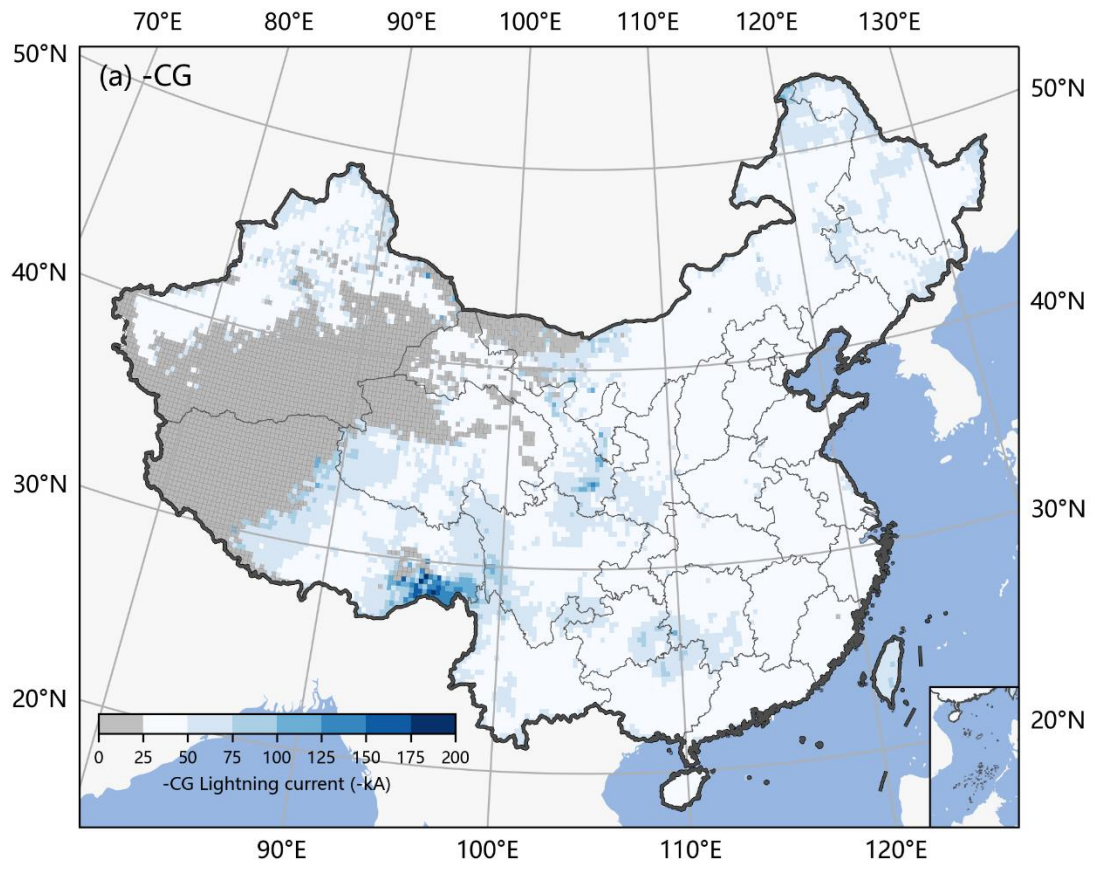


319  
320  
321

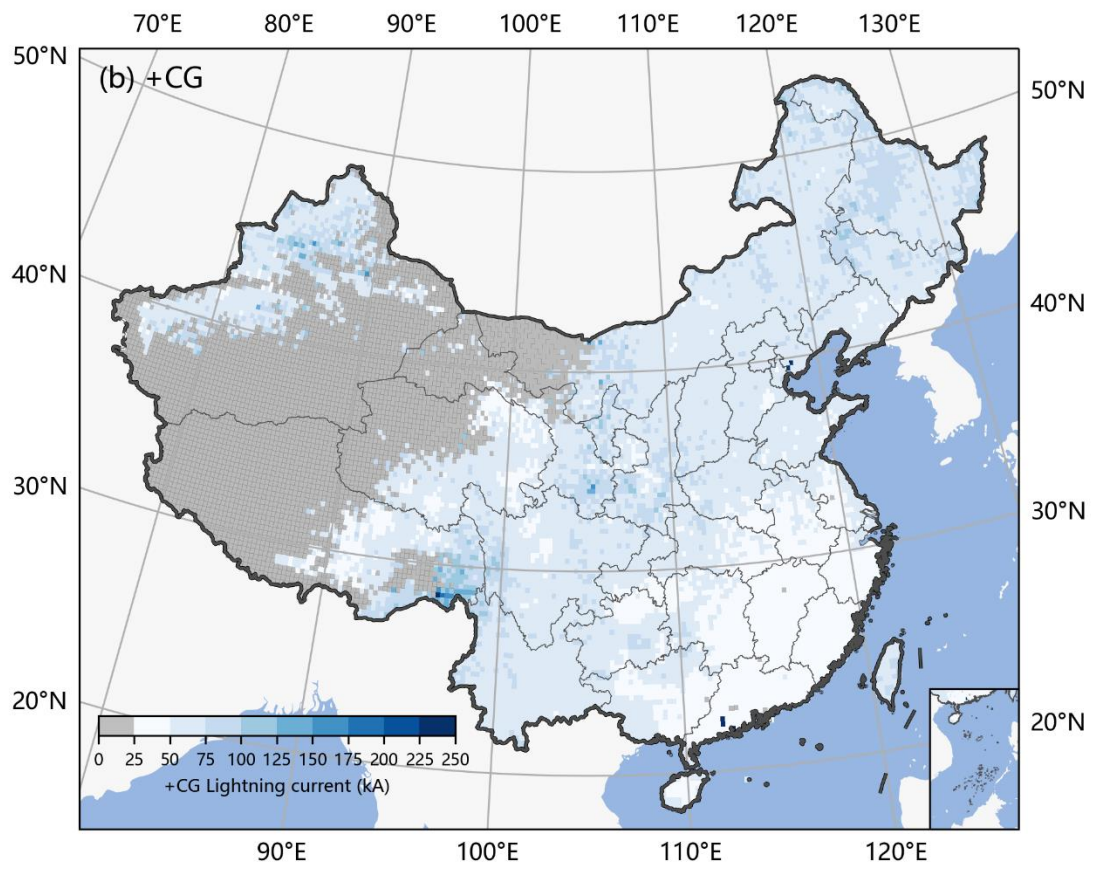
**Fig. 7. Distribution of the proportion of +CG flashes in China. The gray grids have a CG flash number of less than 50 in 6 years and thus are not calculated. The grid size is  $0.25^\circ \times 0.25^\circ$ .**

322  
323  
324  
325  
326  
327  
328  
329

Based on Fig. 8, it can be inferred that the spatial distribution of the current values for both +CG and -CG is generally similar, with lower current values observed in the southeast, where lightning activity is more frequent, and higher current values found in other inland areas. Notably, the current values in southern Gansu, the plain in Médog County, and the intersection of Guizhou, Hunan, and Guangxi are higher, where the proportion of +CG is also relatively high. Therefore, it can be concluded that a high proportion of +CG typically corresponds to larger current values in terms of temporal and spatial scales.



330



331

332  
333  
334

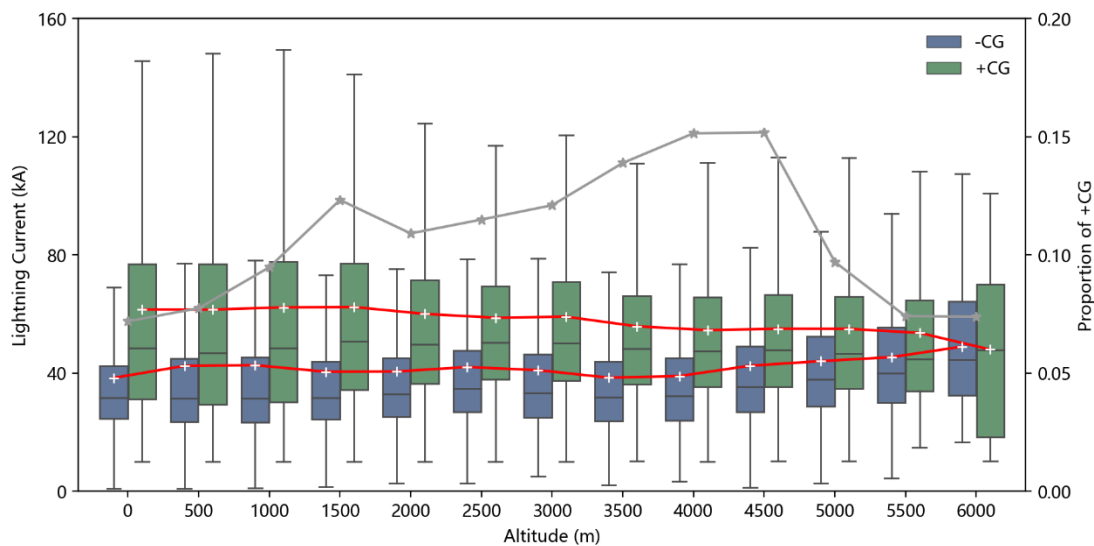
**Fig. 8. Distribution of the average peak current of (a) -CG and (b) +CG flashes in China. The gray grids have a -CG or +CG flash number of less than 50 in 6 years and thus are not calculated. The grid size is  $0.25^\circ \times 0.25^\circ$ .**

335  
336  
337  
338  
339  
340  
341  
342  
343

The proportion of +CG flashes in different altitude layers is calculated, as shown by the gray line in Fig. 9. Below 4500 meters altitude, the proportion increases with altitude, ranging from 7% to 15%. A sub-peak is observed at 1500 meters, which is caused by the high proportion region of +CG lightning flashes in Xinjiang and Inner Mongolia. However, above 4500 meters altitude, which mainly comprises the uninhabited areas of the western and northern Tibetan Plateau, the proportion of +CG lightning flashes decreases rapidly. It is worth noting that only 91 CG flashes occurred above 6000 meters of altitude during the six-year period and are not included in the statistics.

344  
345  
346  
347  
348  
349  
350  
351  
352  
353

The box plot in Fig. 9 shows the current distribution of +CG and -CG lightning flashes at different altitudes. The distribution of lightning current decreases with increasing altitude. Interestingly, the average current of -CG lightning flashes shows a slight positive correlation with altitude, whereas +CG lightning flashes exhibit a negative correlation with altitude. The opposite trend of the two types of lightning flashes leads to a large difference in their discharge intensity at low altitudes and coincidence at high altitudes. Most of the reasons for the complexity of lightning activity in China come from the Tibetan Plateau, the "third pole" of the Earth, where the charge structure of thunderstorm clouds has some special characteristics due to the high-altitude ground surface(Li et al., 2013; Qie et al., 2005).



354  
355

**Fig. 9. The peak current distribution of +CG and -CG and the proportion of +CG versus altitude**

#### 356 4. Conclusion

357  
358

China is primarily located in temperate and subtropical zones, with climate subject to a variety of factors, including cold and warm monsoons, the interplay of land and

---

359 sea, and varied topography. As a result, there are frequent convective weathers and a  
360 high prevalence of lightning activities. This paper utilizes the dataset from a ground-  
361 based lightning location system, CNLDN, which has relatively higher detection  
362 efficiency and smaller location errors for CG lightning compared with other national  
363 networks and the Lightning Mapping Imager on FY-4A satellite, to analyze the CG  
364 lightning characteristics in China over the past six years. The spatial and temporal  
365 distribution of +CG and -CG lightning exhibit regular patterns in terms of their  
366 frequency, ratio, and discharge intensity.

367 The results indicate that there are more CG lightning flashes in southern regions  
368 than in northern regions, more in mountainous areas than in plains at the same latitude,  
369 more in humid areas than in arid areas, and more in coastal areas than in inland areas  
370 within the same climate zone. The southeast coastland of China has the highest CG  
371 lightning density, while the northwest deserts and basins as well as the east and north  
372 Tibetan Plateau have the lowest density. The monsoon system plays a critical role in  
373 lightning activities in southern and Northern China, while the Tibetan Plateau  
374 contributes to the complexity of lightning activities in Northwestern China and the  
375 Qinghai-Tibet region. Overall, the distribution of lightning activity across China is  
376 consistent with the precipitation distribution observed at a climatic scale.

377 In general, +CG flashes have a lower occurrence rate than -CG flashes, but they  
378 carry higher currents and are more destructive. The spatial and temporal distribution of  
379 +CG and -CG flashes also varies significantly due to their different mechanisms. The  
380 lightning activity follows a seasonal pattern, with the highest frequency occurring  
381 during summer (70.7%), followed by spring (19.1%) and autumn (9.8%), and the least  
382 frequent in winter (0.4%). In spring, autumn, and winter, lightning is mainly  
383 concentrated in the southeastern coastal areas. The percentage of +CG flashes is  
384 inversely correlated with lightning frequency. High lightning frequency in summer  
385 generally corresponds to a low proportion of +CG flashes, while low frequency in  
386 winter corresponds to a high proportion of +CG flashes. The proportion of +CG flashes  
387 in winter thunderstorms in the eastern part of the Qinghai-Tibet Plateau is the highest,  
388 reaching up to 55%. The average discharge intensity of lightning is strongly correlated  
389 with the proportion of +CG flashes and also follows a seasonal pattern of being high in  
390 winter and low in summer. The seasonal fluctuations of +CG flashes are stronger than  
391 -CG flashes. In Southern China, the average intensity of +CG flashes in summer is even  
392 below -CG flashes. On the hourly scale, lightning is active in the late afternoon and  
393 midnight, with a peak between 15:00-17:00 CNT and drop to a trough the following  
394 day between 8:00-10:00 CNT. The proportion of +CG flashes throughout the day  
395 follows an inverse trend with the frequency of lightning, but the minimum proportion  
396 occurs 2-3 hours earlier than the maximum frequency. The highest proportion of +CG  
397 at low latitudes always occurs in the morning, while at high latitudes, it tends to occur  
398 at midnight. The changes in discharge intensity during the day at high latitudes are not  
399 significant. In Southern China, the discharge intensity of +CG and -CG flashes drops  
400 significantly at noon and afternoon, with +CG current dropping even lower than -CG



---

401 current.

402 The distribution of the +CG proportion exhibits significant spatial variability. In  
403 Southern China, where the density of CG lightning is the highest, the +CG proportion  
404 is the lowest, at less than 10%. In contrast, the high-latitude regions such as the North  
405 China Plain, Inner Mongolia, and northern and central Xinjiang have a much higher  
406 proportion of 30-40%. The proportion of +CG lightning below 4500 meters is positively  
407 correlated with altitude and drops sharply after exceeding 4500 meters in the western  
408 and northern regions of the Tibetan Plateau. The spatial distribution of discharge  
409 intensity of +CG and -CG is consistent, and a higher proportion of +CG lightning is  
410 generally associated with greater discharge intensity for both types. As latitude  
411 increases, the current distribution widens. The discharge intensity of +CG lightning  
412 shows a slight decrease with increasing altitude, while the intensity of -CG increases  
413 with altitude. Consequently, there is a significant difference in discharge intensities  
414 between the two types at low altitudes, but they tend to be similar at higher altitudes.

415 The lightning location system sites cannot be evenly distributed due to geographic  
416 factors, thus bringing about errors in lightning distribution analysis. The observation  
417 from the Lightning Mapping Imager (LMI) on the FY-4A satellite will be used to correct  
418 the distribution deviations by ground-based data in our following research. Given the  
419 vast size of China, a simple division into four regions may be too crude to study the  
420 influence of geographic and climatic factors on CG lightning characteristics in depth.  
421 Therefore, a more detailed division will be necessary for future studies.

## 422 Acknowledgments:

423 This study is supported by the Key Technologies Research and Development  
424 Program of China (2020YFB1600103). We appreciate the Meteorological Observation  
425 Centre of CMA and the Institute of Electrical Engineering of CAS for their data support.  
426 We also thank the reviewers and editors for their valuable suggestions for this study.

## 427 Reference

428 Carey, L. D. and Buffalo, K. M.: Environmental control of cloud-to-ground lightning polarity in  
429 severe storms, *Monthly Weather Review*, 135, 1327---1353, 2007.

430 Cummins, K. L., Murphy, M. J., Bardo, E. A., Hiscox, W. L., Pyle, R. B., and Pifer, A. E.: A  
431 combined TOA/MDF technology upgrade of the US National Lightning Detection Network, *Journal of*  
432 *Geophysical Research: Atmospheres*, 103, 9035-9044, 1998.

433 Jin, H., Chen, X., Wu, P., Song, C., and Xia, W.: Evaluation of spatial-temporal distribution of  
434 precipitation in mainland China by statistic and clustering methods, *Atmospheric Research*, 262, 105772,  
435 2021.

436 Li, P., Zhai, G., Pang, W., Hui, W., Zhang, W., Chen, J., and Zhang, L.: Preliminary research on a  
437 comparison and evaluation of FY-4A LMI and ADTD data through a moving amplification matching  
438 algorithm, *Remote Sensing*, 13, 11, 2020.

---

439 Li, Y., Zhang, G., Wen, J., Wang, D., Wang, Y., Zhang, T., Fan, X., and Wu, B.: Electrical structure  
440 of a Qinghai–Tibet Plateau thunderstorm based on three-dimensional lightning mapping, *Atmospheric*  
441 *Research*, 134, 137-149, 2013.

442 Liu, Y., Wang, H., Li, Z., and Wang, Z.: A verification of the lightning detection data from FY-4A  
443 LMI as compared with ADTD-2, *Atmospheric Research*, 248, 105163, 2021.

444 Ma, M., Tao, S., Zhu, B., and Lü, W.: Climatological distribution of lightning density observed by  
445 satellites in China and its circumjacent regions, *Science in China Series D: Earth Sciences*, 48, 219-229,  
446 2005.

447 Ma, R., Zheng, D., Zhang, Y., Yao, W., Zhang, W., and Cuomu, D.: Spatiotemporal Lightning  
448 Activity Detected by WWLLN over the Tibetan Plateau and Its Comparison with LIS Lightning, *Journal*  
449 *of Atmospheric and Oceanic Technology*, 38, 511-523, 2021.

450 Nag, A., Rakov, V. A., and Cummins, K. L.: Positive Lightning Peak Currents Reported by the U.S.  
451 National Lightning Detection Network, *IEEE Transactions on Electromagnetic Compatibility*, 56, 404-  
452 412, 2014.

453 Preston and Tolver, S.: The lightning discharge, *Philosophical Magazine Series 1*, 31, 443-445, 1989.

454 Qie, X., Toumi, R., and Zhou, Y.: Lightning activity on the central Tibetan Plateau and its response  
455 to convective available potential energy, *Chinese Science Bulletin*, 48, 296-299, 2003.

456 Qie, X., Zhang, T., Chen, C., Zhang, G., Zhang, T., and Wei, W.: The lower positive charge center  
457 and its effect on lightning discharges on the Tibetan Plateau, *Geophysical research letters*, 32, 2005.

458 Rakov, V. A. and Uman, M. A.: *Lightning: Physics and Effects*, *Lightning: Physics and Effects*2003.

459 Ren, G., Ding, Y., Zhao, Z., Zheng, J., Wu, T., Tang, G., and Xu, Y.: Recent progress in studies of  
460 climate change in China, *Advances in Atmospheric Sciences*, 29, 958-977, 2012.

461 Schulz, W., Diendorfer, G., Pedeboy, S., and Poelman, D. R.: The European lightning location  
462 system EUCLID–Part 1: Performance analysis and validation, *Natural Hazards and Earth System*  
463 *Sciences*, 16, 595-605, 2016.

464 Wang, J., Huang, Q., Ma, Q., Chang, S., He, J., Wang, H., Zhou, X., Xiao, F., and Gao, C.:  
465 Classification of VLF/LF Lightning Signals Using Sensors and Deep Learning Methods, *Sensors (Basel,*  
466 *Switzerland)*, 20, 2020.

467 Williams, E. R.: Large - scale charge separation in thunderclouds, *Journal of Geophysical Research:*  
468 *Atmospheres*, 90, 6013-6025, 1985.

469 You, J., Zheng, D., Zhang, Y., Yao, W., and Meng, Q.: Duration, spatial size and radiance of lightning  
470 flashes over the Asia-Pacific region based on TRMM/LIS observations, *Atmospheric Research*, 223, 98-  
471 113, 2019.

472